



Bis-guanylhydrazones as efficient anti-*Candida* compounds through DNA interaction

Jelena Lazić^{1,2} · Vladimir Ajdačić¹ · Sandra Vojnović² · Mario Zlatović¹ · Marina Pekmezović³ · Selene Mogavero³ · Igor Opsenica¹ · Jasmina Nikodinovic-Runic²

Received: 25 August 2017 / Revised: 25 December 2017 / Accepted: 27 December 2017 / Published online: 12 January 2018
© Springer-Verlag GmbH Germany, part of Springer Nature 2018

Abstract

Candida spp. are leading causes of opportunistic mycoses, including life-threatening hospital-borne infections, and novel antifungals, preferably aiming targets that have not been used before, are constantly needed. Hydrazone- and guanidine-containing molecules have shown a wide range of biological activities, including recently described excellent antifungal properties. In this study, four bis-guanylhydrazone derivatives (BG1–4) were generated following a previously developed synthetic route. Anti-*Candida* (two *C. albicans*, *C. glabrata*, and *C. parapsilosis*) minimal inhibitory concentrations (MICs) of bis-guanylhydrazones were between 2 and 15.6 µg/mL. They were also effective against preformed 48-h-old *C. albicans* biofilms. In vitro DNA interaction, circular dichroism, and molecular docking analysis showed the great ability of these compounds to bind fungal DNA. Competition with DNA-binding stain, exposure of phosphatidylserine at the outer layer of the cytoplasmic membrane, and activation of metacaspases were shown for BG3. This pro-apoptotic effect of BG3 was only partially due to the accumulation of reactive oxygen species in *C. albicans*, as only twofold MIC and higher concentrations of BG3 caused depolarization of mitochondrial membrane which was accompanied by the decrease of the activity of fungal mitochondrial dehydrogenases, while the activity of oxidative stress response enzymes glutathione reductase and catalase was not significantly affected. BG3 showed synergistic activity with amphotericin B with a fractional inhibitory concentration index of 0.5. It also exerted low cytotoxicity and the ability to inhibit epithelial cell (TR146) invasion and damage by virulent *C. albicans* SC5314. With further developments, BG3 may further progress in the antifungal pipeline as a DNA-targeting agent.

Keywords Antifungal activity · *Candida* spp. · Bis-guanylhydrazone · DNA interaction · ROS generation · Synergy

Introduction

The incidence and severity of fungal diseases has increased worldwide, with mortality caused by invasive fungal

infections remaining disturbingly high. Invasive fungal infections are regarded as “hidden killers” resulting in over 1,350,000 deaths every year (Brown et al. 2012a). The high rates of morbidity and mortality caused by fungal infections have been associated with the currently limited number of antifungal agents and their corresponding fungal targets, the high toxicity of these compounds, and the emergence of drug-resistant fungal strains (Denning and Bromley 2015; Denning et al. 2017; Scorzoni et al. 2017).

Candida albicans is one of the leading opportunistic fungal pathogens, still responsible for more than 50% of human candidiasis, that has usually been associated with high-risk patient populations, such as neonates or cancer and surgical patients (Bassetti et al. 2016; van der Meer et al. 2010). However, during recent years, candidaemia has emerged as a rising problem in other, more general, patient groups, while a shift in species distribution towards an increasing prevalence of

Electronic supplementary material The online version of this article (<https://doi.org/10.1007/s00253-018-8749-3>) contains supplementary material, which is available to authorized users.

✉ Igor Opsenica
igorop@chem.bg.ac.rs

✉ Jasmina Nikodinovic-Runic
jasmina.nikodinovic@imgge.bg.ac.rs

¹ Faculty of Chemistry, University of Belgrade, Studentski trg 16, P.O. Box 51, Belgrade 11158, Serbia

² Institute of Molecular Genetics and Genetic Engineering, University of Belgrade, Vojvode Stepe 444a, Belgrade 11000, Serbia

³ Department of Microbial Pathogenicity Mechanisms, Hans Knöll Institute, Jena, Germany

Candida glabrata and *Candida parapsilosis* has also been documented (Guinea 2014; Silva et al. 2012). When given the opportunity, *C. albicans* can proliferate and invade virtually any site in the host due to numerous virulence factors. Among these, the ability to form highly resistant biofilms on a variety of inert and biological surfaces contributes greatly to *C. albicans* pathogenesis (Tsui et al. 2016; Wu et al. 2017).

The antifungal research field is dynamic (Calderone et al. 2014; Godoy et al. 2016; Ngo et al. 2016); however, the most recent reality check of the fungal pipeline (Perfect 2017) has pointed out that a greater effort should be put into the discovery and development of new antifungal agents and strategies in order to secure more successful management of invasive fungal infections in the future. In order to stay ahead in the arms race against fungal resistance, there is a constant need to identify new antifungals and one strategy to achieve; that is to aim for targets that have not been fully used before. For instance, DNA as a target is rather underexplored for antimicrobials, especially antifungals (Bolhuis and Aldrich-Wright 2014).

In recent advances, various heterocycles, including imidazole, benzimidazole, and more than 20 other heterocyclic scaffolds, have been identified as potential antifungal leads (Kathiravan et al. 2012). Hydrazone- and guanidine-containing molecules have shown a wide range of other biological activities, including recently described excellent antifungal properties (Ajdačić et al. 2016; Shrestha et al. 2017). Previous work from our laboratory has explored the antifungal effect of the series of guanylhydrazones and found that the only bis-guanylhydrazone derivative containing two guanylhydrazone (amidinohydrazone) functional groups showed potent broad-spectrum antifungal activity and favorable cytotoxicity and embryo toxicity profile (Ajdačić et al. 2016). Following up on these findings, we have generated and characterized three novel bis-guanylhydrazones and we have assessed their anti-*Candida* spp. potential. In addition, we evaluated DNA as an initial target of action and examined their potential to cause oxidative stress.

Materials and methods

Synthesis of BG1–4

Bis-guanylhydrazones BG1–4 were obtained in good to high yields using a straightforward, previously reported procedure (Fig. S1 and Fig. S2) (Ajdačić et al. 2016). Characterization of the new compounds has been done by nuclear magnetic resonance (NMR) and mass spectroscopy (Supporting material).

Antimicrobial susceptibility testing

Stock solutions of BG1–4 were prepared in dimethyl sulfoxide (DMSO; 50 mg/mL). Control compounds amphotericin B

(AmB; Sigma-Aldrich, Munich, Germany), nystatin (NYS; Acros Organics, Geel, Belgium), and kanamycin (KAN; Sigma-Aldrich, Munich, Germany) were dissolved in DMSO (AmB and NYS) and water (KAN) in a concentration of 50 mg/mL. Stock solutions were prepared fresh and kept at 4 °C prior to use.

Minimal inhibitory concentration (MIC) values against *Pseudomonas aeruginosa* NCTC 10332, *Staphylococcus aureus* ATCC 25923, *Micrococcus luteus* ATCC 379, and *Listeria monocytogenes* NCTC 11994 were determined in Luria-Bertani broth (10 g/L tryptone, 10 g/L NaCl, 5 g/L yeast extract, pH 7.2) in accordance with the standard broth microdilution assay for bacteria that grow aerobically, as recommended by the CLSI (Clinical and Laboratory Standards Institute 2015). The highest tested concentration of BG1–4 was 500 µg/mL, and the inocula were 1×10^6 colony forming units (cfu)/mL.

Susceptibility testing of *Candida* spp. (*C. albicans* ATCC 1023, *C. albicans* SC5314 (ATCC MYA-2876), *C. parapsilosis* ATCC 22019, and *C. glabrata* ATCC 2001) was performed according to the CLSI broth microdilution guidelines (Clinical and Laboratory Standards Institute 2008; Clinical and Laboratory Standards Institute 2012), in Sabouraud broth (10 g/L peptone, 40 g/L dextrose, pH 5.6). The highest tested concentration of BG1–4 was 500 µg/mL, and the inocula were 1×10^5 cfu/mL.

MIC values were read after 24 h of incubation at 37 °C as the lowest concentration to exhibit the absence of growth.

Biofilm inhibition and dispersion assays

Wild-type strain *C. albicans* SC5314 was used for antibiofilm assays as previously described (Ajdačić et al. 2016; Pierce et al. 2008), with minor modifications. Cells were harvested from overnight grown cultures (Sabouraud broth, 180 rpm, 30 °C) by centrifugation ($5000 \times g$, 5 min, 4 °C), washed twice with sterile phosphate-buffered saline (PBS; Sigma-Aldrich, Munich, Germany), and resuspended in RPMI 1640 medium (Sigma-Aldrich) supplemented with L-glutamine and containing 2% glucose (w/v) at a concentration of 2×10^6 cells/mL. In the biofilm inhibition assay, 100 µL of compounds BG1–4 at various concentrations in RPMI 1640 medium was added to each well of a 96-well polystyrene, round-bottom plate followed by 100 µL of inoculum and the plates were incubated at 37 °C for 48 h to allow biofilm formation.

In the biofilm dispersion assay, biofilms were formed in 96-well microtiter plates during 48 h of incubation (without shaking) at 37 °C. After the incubation period, the wells were washed twice with PBS to remove any non-adherent cells and twofold serial dilutions of BG1–4 in 200 µL fresh RPMI medium were added to the wells containing preformed biofilms. The biofilms were then incubated in the presence of compounds for an additional period of 24 h.

Biofilm growth was analyzed by crystal violet (CV) staining of adherent cells, and the absorbance at 590 nm was read on a Tecan Infinite 200 Pro multiplate reader (Tecan Group Ltd., Männedorf, Switzerland).

In vitro cytotoxicity

Antiproliferative activities of BG1–4 were measured using the standard colorimetric MTT [3-(4,5-dimethylthiazol-2-yl)-2,5-diphenyltetrazolium bromide] assay (Hansen et al. 1989). MRC5 cells (human lung fibroblast, obtained from ATCC) were plated in a 96-well flat-bottom plate at a concentration of 1×10^4 cells per well, grown in humidified atmosphere of 95% air and 5% CO₂ at 37 °C, and maintained as monolayer cultures in RPMI 1640 medium. Each tested compound was added to the cells at a concentration of 0.5–250 µg/mL, and the treatment lasted for 48 h. The MTT assay was performed two times in four replicates, and the results were presented as percentage of the DMSO-treated control that was arbitrarily set to 100%. The percentage viability values were plotted against the log of concentration, and a sigmoidal dose-response curve was calculated by non-linear regression analysis using GraphPad Prism software version 5.0 for Windows (GraphPad Software, CA, USA). From these curves, IC₅₀ (concentration causing 50% cell death) values were obtained.

In vitro DNA interaction assays and molecular modeling

DNA from *C. albicans* and pUC19 plasmid DNA was purified with a QIAamp[®] DNA Mini Kit (Qiagen, Hilden, Germany). For the gel electrophoresis experiments, genomic DNA (750 ng) was treated with the compounds BG1–4 (40, 200, and 1000 µg/mL) in 20 µL of water for 30 min at 37 °C.

The ability of BG1–4 to cleave DNA was examined by following the conversion of the supercoiled form of pUC19 plasmid DNA to the open circular and/or linear forms, also using agarose gel electrophoresis. Plasmid DNA (240 ng) was treated with the BG1–4 (0.1 and 0.5 µM which is equal to 40 and 200 µg/mL) in 20 µL water for 1 h at 37 °C.

After incubation, reaction mixtures were subjected to electrophoresis on a 0.8% (*w/v*) agarose gel containing 0.1 mg/L of ethidium bromide in TBE buffer (100 mM Tris, 90 mM boric acid, 1 mM EDTA, pH 7.4) at 60 V for 1.5 h. Gels were visualized and analyzed using the Gel Doc EZ system (Bio-Rad, Life Sciences, Hercules, USA), equipped with the Image Lab[™] software.

CD spectra of commercially available double-stranded template DNA (dsDNA) isolated from herring sperm (Boehringer Mannheim GmbH, Germany) and its complexes with various amounts of BG1–4 (0–50 µM) were recorded on a Jasco J-815 circular dichroism spectropolarimeter (Jasco, UK) calibrated with ammonium (+)-10-camphorsulfonate.

Spectra were recorded over a wavelength range of 220–320 nm in 0.1-nm steps at an instrument scanning rate of 200 nm/min using a quartz cell of 0.1 mm optical path length and with a data integration time of 2 s. The reported spectra represent the average of three scans at 25 °C. The results are expressed as ellipticity, measured in mdeg.

For DNA docking simulations, the crystal structure of dodecamer PDB ID: 3U2N [d(CGCGAATTCGCG)₂] was obtained from the Protein Data Bank (<http://www.rcsb.org/pdb>) (Wei et al. 2013). All water molecules and ions as well as ligands were removed using AutoDock Tools 1.5.6 (Morris et al. 2009; Sanner 1999). Bis-guanyldiazone molecules were prepared using Maestro 10.4 from the Schrödinger Suite 2015-4 (Maestro, version 10.4, Schrödinger, LLC, New York, 2015). All possible tautomer structures at pH 7.00 ± 2.00 were generated using Epik 3.4 from the Schrödinger Suite 2015-4 (Epik, version 3.4, Schrödinger, LLC, New York, 2015), and their charges were determined in Jaguar 9.0 (Jaguar, version 9.0, Schrödinger, LLC, New York, 2015) using the HF/6-31g* method. These charges were used further in docking simulations. The docking simulations were realized in AutoDock Vina 1.1.2 (Trott and Olson 2010). The grid box size was set to 24 × 28 × 40 Å³ and exhaustiveness to 500. For every molecule, docking was repeated four times, and best ranked structures were examined. Discovery Studio Visualizer 4.5 was used for visualization of the interactions (Dassault Systèmes BIOVIA, Discovery Studio Modeling Environment, release 4.5, San Diego, USA, 2015).

DNA-binding fluorescent staining and microscopy

Overnight *C. albicans* culture was diluted to OD₆₀₀ = 0.6 and incubated with 1 × MIC of the compounds BG1–4 and 1 µg/mL of AmB for 3 h at 30 °C. The control was incubated with DMSO. After completion of the incubation period, cells were diluted to 1×10^7 cells/mL, washed twice with PBS, and stained with 1 µg/mL of 2-(4-amidinophenyl)-6-indolecarbamidine dihydrochloride (DAPI; Sigma-Aldrich, Munich, Germany) in PBS in an orbital shaker (180 rpm) at 30 °C for 10 min in the dark. Cells were visualized using a fluorescence microscope (Olympus BX51, Applied Imaging Corp., San Jose, USA), at a × 60 magnification.

FACS analysis

FITC Annexin V/Dead Cell Apoptosis Kit (Molecular Probes, Invitrogen, Carlsbad, USA) was used for the assessment of cellular integrity and the externalization of phosphatidylserine after treatment of *C. albicans* ATCC 10231 protoplasts with BG3 and AmB using a slightly modified established procedure (Hao et al. 2013).

C. albicans cells (4×10^8) were washed twice in PBS and protoplasted by three-phase incubation at 30 °C for 2 h in

total, in a potassium phosphate (pH 7.2) that contained 10 mg/mL of Proteinase K during the first phase (30 min), dithiothreitol (DTT; 10 mM) and β -mercaptoethanol (30 mM) in the second phase (30 min), and 10 g/L of lysing enzymes from *Trichoderma harzianum* (Sigma-Aldrich) in the last phase (60 min). Protoplast formation was verified by SDS sensitivity (Hazen et al. 1990). Prepared protoplasts were washed and further incubated with 1 \times MIC and 2 \times MIC of BG3 and AmB in the same buffer. Protoplasts were washed in modified annexin binding buffer (10 mM HEPES/NaOH (pH 7.4), 40 mM NaCl, 50 mM CaCl₂, and 1.2 M sorbitol) and stained (2 \times 10⁶ protoplasts) for 20 min in the same buffer containing 5 μ L/mL FITC-annexin and 2.5 μ L/mL of the 100 μ g/mL propidium iodide (PI) solution. The cells were analyzed using a CyFlow Space Partec flow cytometer, with Partec FloMax software (Partec GmbH, Munster, Germany). This experiment was carried out three times independently.

Detection of active *C. albicans* metacaspases was performed using the Intracellular Caspase Detection ApoStat (R&D Systems, Inc., Minneapolis, USA) as previously described (Wu et al. 2010). Briefly, *C. albicans* cells (1 \times 10⁷ cells/mL) treated with 0.5 \times MIC, 1 \times MIC, and 2 \times MIC of BG3 for 3 h were collected, washed in PBS, and stained with 10 μ L of FITC-conjugated V-D-FMK for 30 min at 37 $^{\circ}$ C. After incubation, cells were washed and resuspended in PBS and analyzed using a CyFlow Space Partec flow cytometer, with Partec FloMax software (Partec GmbH, Munster, Germany). This experiment was carried out three times independently.

Intracellular reactive oxygen species (ROS) were measured using the fluorescent dye dihydrorhodamine (DHR-123, Sigma-Aldrich). *C. albicans* cells (1 \times 10⁷ cells) were incubated in an orbital shaker (200 rpm) at 30 $^{\circ}$ C for 3 h in Sabouraud broth with 2 \times MIC of BG3 and 1 \times MIC of AmB. ROS were assessed by the addition of DHR-123 (5 μ g/mL) to treated cells 30 min before the end of each experiment. Cells were then harvested, washed in PBS, and examined by the CyFlow Space Partec flow cytometer.

Assessment of mitochondrial membrane potential ($\Delta\Psi_m$)

$\Delta\Psi_m$ was measured using a JC-1 mitochondrial potential sensor (Molecular Probes, Invitrogen, Carlsbad, USA) with minor modifications to previously published procedure (Guo et al. 2014). *C. albicans* cells (1 \times 10⁷) were stained with 2.5 μ g/mL of JC-1 (5,5',6,6'-tetrachloro-1,1',3,3'-tetraethylbenzimidazol-carbocyanine iodide) at 30 $^{\circ}$ C for 20 min in the dark and washed twice in PBS; treated with 1 \times MIC, 2 \times MIC, and 4 \times MIC of BG3 and 1 \times MIC of AmB; and analyzed using a microtiter plate reader (Tecan Group Ltd., Männedorf, Switzerland) with an excitation wavelength of 490 nm and emission wavelength shifting from

green (530 nm) to red (590 nm) from the start of treatment for 3 h. $\Delta\Psi_m$ was determined as a ratio of red to green fluorescence. A decrease in the ratio was interpreted as a depolarization of mitochondrial membrane potential. In addition, cells were firstly treated with 1 \times MIC, 2 \times MIC, and 4 \times MIC of BG3 followed by JC-1 staining and FACS analysis (CyFlow Space Partec flow cytometer; Partec GmbH, Munster, Germany). Cells prepared in this way were also mounted with 1% low-melting agarose and visualized using a Leica TCS SP8 confocal microscope and Leica Microsystems LAS AF-TCS SP8 software (Leica Microsystems, Wetzlar, Germany) at a \times 62 magnification.

Determination of enzymatic activities

Early-exponential phase *C. albicans* cells (1 \times 10⁷ cells/mL) were treated with 1 \times MIC and 2 \times MIC of BG3 for 3 h at 30 $^{\circ}$ C. Cells were collected by centrifugation, washed in PBS, and resuspended to OD₆₀₀ = 5 in lysis buffer (100 mM Tris-HCl (pH 7.5) and 5 mM DTT, 1 tablet/50 mL Roche Complete protease inhibitor cocktail). Cells were sonicated (5 cycles of 30 s at 11 MHz with 2-min break; MSE Soniprep150 (Sanyo, Osaka, Japan)) and centrifuged at 5000 rpm for 10 min at 4 $^{\circ}$ C (Eppendorf 5417R centrifuge; Eppendorf, Hamburg, Germany), and supernatants were collected and used fresh for the assessment of enzymatic activities. Protein concentration was determined using Quick Start Bradford reagent (Bio-Rad Laboratories, Hercules, USA).

Glutathione reductase and catalase activities were analyzed as previously described (Rowan et al. 2010) using 100 μ L of freshly prepared protein extract, recording absorbance on 340 and 240 nm, respectively, on an Ultrospec 3300Pro spectrophotometer (Amersham Biosciences, Little Chalfont, UK). The activity of mitochondrial dehydrogenases was assessed using XTT (2,3-bis-(2-methoxy-4-nitro-5-sulfophenyl)-2H-tetrazolium-5-carboxanilide) assay as previously described (Wu et al. 2009), recording the absorbance at 490 nm on a Tecan Infinite 200 Pro multiplate reader (Tecan Group Ltd., Männedorf, Switzerland).

Epithelial cell infection model

The ability of *C. albicans* SC5314 cells to infect TR146 epithelial cells (obtained from Cancer Research Technology, London) was tested in the presence of BG3 in the concentration range of 2–16 μ g/mL. More precisely, *C. albicans* cells were co-incubated with oral epithelial cells for 1 h (adhesion assay), 3 h (hyphal length, invasion assay), and 24 h (damage assay) in serum-free Dulbecco's modified Eagle's medium (DMEM; Gibco) at 37 $^{\circ}$ C and 5% CO₂ as described in previous publications (Jakab et al. 2016; Wachtler et al. 2011).

Adherent *C. albicans* cells were stained with calcofluor white (CFW; Sigma-Aldrich) and visualized with a

fluorescence microscope (Leica DM5500B, Leica DFC360 FX). The number of adherent cells was determined by counting of at least 100 high-power fields and expressed as a percentage of adhered cells. In the invasion assay, non-invading *C. albicans* cells were first stained with the Alexa Fluor 488 conjugate of succinylated concanavalin A (ConA; Invitrogen). Afterwards, epithelial cells were permeabilized with 0.5% Triton X-100 and fungal cells were stained with CFW, which allowed differentiation of invading (stained by CFW only) and non-invading (stained by both CFW and ConA) hyphae. The percentage of invading cells and hyphal length were determined using fluorescence microscopy by counting at least 50 invading *Candida* cells. Epithelial cell damage was determined after 24 h of co-incubation by measuring the release of lactate dehydrogenase (LDH) using the LDH cytotoxicity detection kit (Roche Applied Science) according to the manufacturer's instructions. All experiments were performed in triplicates for each condition and repeated three times.

Synergy determination

Fractional inhibitory concentration index (FICI) between BG3 and nystatin, AmB, and itraconazole was determined using the *C. albicans* ATCC 10231 strain and interpreted (synergy – FICI ≤ 0.5 , antagonism – FICI > 4.0 , and no interaction – FICI > 0.5 –4) using the previously described checkerboard microdilution protocol (Odds 2003).

Statistical analysis

Statistical significance was determined by unpaired two-tailed Student's *t* test ($p \leq 0.05$).

Results

Synthesis and characterization of BG1–BG4

Preparation of the bis-guanylhydrazones BG1–4 (Fig. 1) was accomplished by reaction of dialdehydes with aminoguanidine hydrochloride (Fig. S1 and Fig. S2). Their spectral characteristics are given in the [Supplementary data](#). In comparison to BG1, additional methyl groups were introduced in BG2, the heteroatom of the central core was replaced in BG3, and the additional heteroatom as well as the phenyl group were introduced in BG4 (Fig. 1).

Antimicrobial and cytotoxic properties of BG1–4

Bis-guanylhydrazones BG1–4 showed substantially higher anti-*Candida* spp. activities in comparison to those against bacterial species (Table 1). MICs against bacterial strains were mostly ≥ 500 $\mu\text{g/mL}$, while anti-*Candida* MICs were in the

range of 2–15.62 $\mu\text{g/mL}$. The most sensitive was *C. parapsilosis*, with MIC values of BG1–4 being comparable with those of nystatin. Cytotoxicity against healthy human fibroblasts (MRC5) of these compounds was between 10 and 40 $\mu\text{g/mL}$, implying moderate selectivity index. However, the derivative BG3 showed the lowest cytotoxicity and the highest antifungal activity with the selectivity indexes between 10 and 20 (Table 1).

Effect of BG1–BG4 on *C. albicans* SC5314 biofilms

In the standard 96-well plate assays, it was shown that bis-guanylhydrazones BG1–4 had good antibiofilm formation properties but, virtually, no ability to disperse preformed *Candida* biofilms (Table 2). BG2 showed the best biofilm-inhibiting potential with the complete biofilm inhibition activity achieved at between 2- and 30-fold higher concentrations in comparison to MIC values against planktonic cells (Table 1). This is important, as some known antifungal drugs including fluconazole showed biofilm inhibition at concentrations > 1000 -fold compared to its activity against the minor activity of planktonic counterparts on biofilm dispersion (Maiolo et al. 2014; Uppuluri et al. 2011).

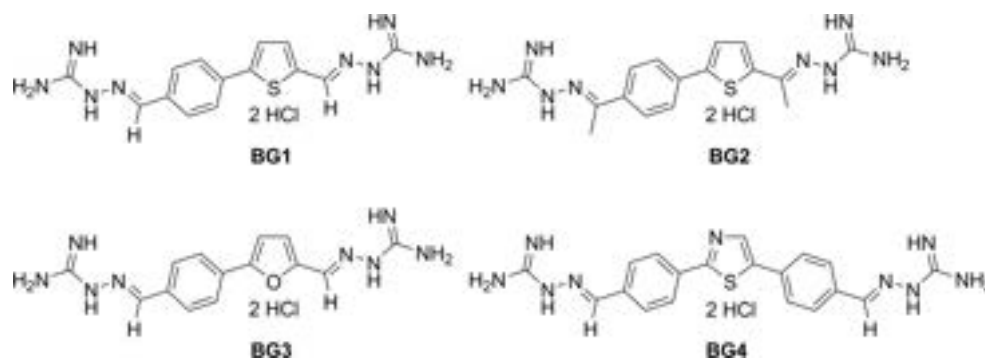
DNA interaction ability of BG1–4

To determine the basis for growth inhibition of *Candida* spp. by BG1–4 and their initial target site, the potential to interact with chromosomal DNA from *C. albicans* was assessed (Fig. 2). This approach was based on our earlier observation that BG1 efficiently interacted with DNA, while fungal membrane as the primary activity site was excluded by the inability of this compound to disrupt unilamellar liposomes containing ergosterol, thus mimicking fungal membranes (Ajdačić et al. 2016).

In this experiment, purified DNA from *C. albicans* was incubated with various concentrations of BG1–4 compounds and visualized by ethidium bromide staining. The excellent ability of bis-guanylhydrazones to interact with high molecular weight double-stranded DNA (BG3 $>$ BG1 $>$ BG2 $>$ BG4) resulted in the inability of ethidium bromide to intercalate and emit under UV exposure (Fig. 2). Importantly, this interaction did not cause DNA degradation. The same DNA interaction trend was observed when the substrate was supercoiled plasmid pUC19 DNA, where neither cleavage nor linearization has been observed, but the interaction led to a decrease in fluorescence intensity of the ethidium bromide-DNA complex (Fig. S3).

Further in vitro evidence of the DNA interaction ability of BG1–4 was obtained from the circular dichroism (CD) spectral analysis and molecular modeling (Fig. 2 and Fig. S4). The CD spectrum of the dsDNA isolated from herring sperm shows a maximum at 277 nm, due to base stacking, and a minimum at 245 nm, which is attributed to the right-handed helicity of the B-type DNA. Figure 3a depicts the CD spectra of dsDNA

Fig. 1 Chemical structures of bis-guanylhydrazones BG1–4



solution at different ratios with bis-guanylhydrazone BG3, as well as the CD spectrum of DNA and BG3 alone. With the increasing concentrations of the compound, both positive and negative peaks decreased in ellipticity and intensity in a concentration-dependent manner. An evident blue shift is obtained for positive bands. This indicated that the interaction between BG3 and DNA significantly perturbs the conformation of the dsDNA. Given that intercalation significantly enhances the intensities of both the positive and negative peaks as a result of stabilization of the B-DNA conformation, it could be concluded that the bis-guanylhydrazones do not bind to dsDNA by typical intercalation (Fig. 3a, Fig. S4). CD spectra of bis-guanylhydrazone BG4 revealed that the conformation changes of the dsDNA induced by this derivative were less remarkable in line with results obtained by gel electrophoresis experiments (Fig. 2, Fig. S4e).

The molecular docking calculations performed for BG1–4 using the DNA sequence PDB ID: 3U2N [d(CGCGAATT CGCG)₂], as a substrate, suggested binding to the minor groove as the likely mode of DNA interactions for BG1–4. No intercalating structures were found. The pattern of binding of BG3 is presented in Fig. 3b. The established interactions between the molecule and DNA nucleotides are predominantly hydrogen bonds and some carbon–hydrogen bonding, π –

alkyl interactions, and electrostatic interactions with the phosphodiester groups.

Pro-apoptotic effect of BG3 on *C. albicans*

It has been suggested that apoptotic proteins might be suitable targets for novel antifungal treatments; thus, we have examined the ability of the most potent bis-guanylhydrazone to cause apoptosis in *C. albicans* using fluorescent probes and flow cytometry (Fig. 4).

DAPI is a widely used DNA-specific probe which forms a fluorescent complex by attaching in the minor groove of A-T-rich sequences of DNA and also forms intercalative complexes with double-stranded nucleic acids (Beccia et al. 2012). DAPI easily passes the membrane and strongly binds to DNA of both living and dead cells (giving blue fluorescence with $\lambda_{\max} = 461$ nm). When *C. albicans* resting cells were treated with MICs of BG3 and AmB for 3 h and stained with DAPI, it was obvious that the intensity of blue color of the DNA-DAPI complexes was substantially lower in *C. albicans* cells treated with BG3 in comparison to DMSO- or AmB-treated cells (Fig. 4a). This further confirmed that BG3 competitively prevented the binding of DAPI stain to DNA. The presence of irregular, non-spherical condensed

Table 1 Minimal inhibitory concentrations (MICs) against bacterial and fungal strains and IC₅₀ against human fibroblasts of bis-guanylhydrazones and standard antibiotics ($\mu\text{g}/\text{mL}$)

| Strain/cell line | MIC ($\mu\text{g}/\text{mL}$) | | | | | | |
|------------------------------------|---------------------------------|-------|-------|-------|-------|------|------|
| | Compound | | | | | | |
| | BG1 | BG2 | BG3 | BG4 | KAN | NYS | AmB |
| <i>P. aeruginosa</i> NCTC 10332 | 250 | 500 | 250 | > 500 | 50 | – | – |
| <i>S. aureus</i> ATCC 25923 | > 500 | > 500 | > 500 | > 500 | 10 | – | – |
| <i>M. luteus</i> ATCC 379 | 62.50 | 250 | 250 | 500 | 12.50 | – | – |
| <i>L. monocytogenes</i> NCTC 11994 | > 500 | > 500 | 250 | > 500 | 12.50 | – | – |
| <i>C. albicans</i> ATCC 10231 | 6.25 | 6.25 | 3.13 | 4 | – | 1.00 | 1.00 |
| <i>C. albicans</i> SC5314 | 15.62 | 6.25 | 4 | 6.25 | – | 2.50 | 3.13 |
| <i>C. glabrata</i> ATCC 2001 | 15.62 | 3.13 | 3.13 | 12.50 | – | 2.50 | 1.00 |
| <i>C. parapsilosis</i> ATCC 22019 | 2 | 6.2 | 2 | 3.13 | – | 2.00 | 1.25 |
| MRC5 | 10 | 25 | 40 | 10 | – | – | – |

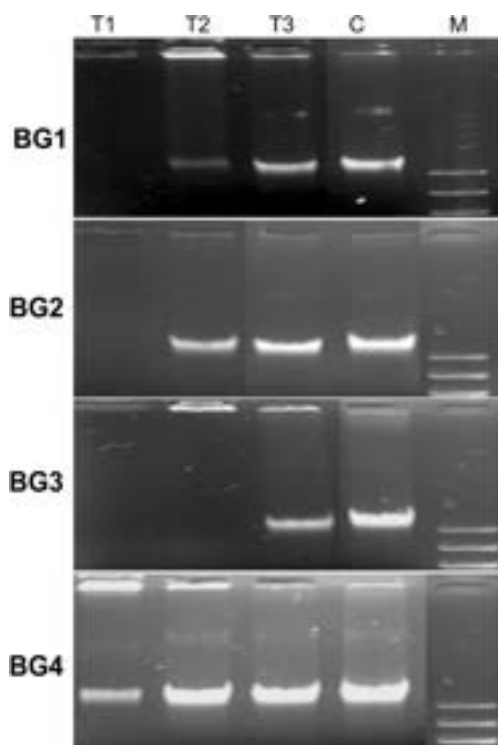
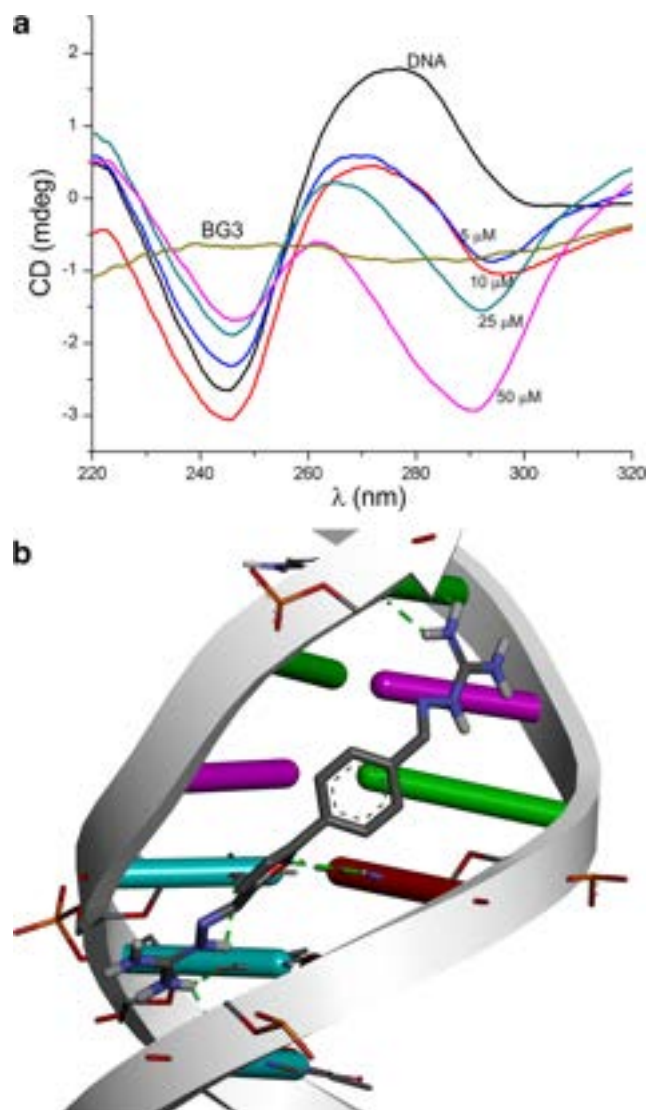
KAN kanamycin, NYS nystatin, AmB amphotericin B

Table 2 Antibiofilm activity (inhibition of the formation and disruption of preformed biofilms) of BG1–4 given in micrograms per milliliter using *C. albicans* SC5314

| Compound | Inhibition of biofilm formation | Disruption of preformed biofilm |
|----------|---------------------------------|---------------------------------|
| BG1 | 62.50 | > 500 |
| BG2 | 15.62 | > 500 |
| BG3 | 31.25 | > 500 |
| BG4 | 125 | 250 |

nuclei indicated apoptosis, which was much more pronounced in AmB-treated cells under tested conditions.

Flow cytometry analysis of apoptotic markers in *C. albicans* protoplasts revealed the induction of apoptosis triggered by BG3 and confirmed it for the AmB (Phillips et al. 2003) (Fig. 4b). The exposure of *C. albicans* protoplasts to both BG3 and AmB resulted in a similar level of increase of early (annexin V⁺/PI⁻) and late (annexin V⁺/PI⁺) apoptotic protoplasts compared to control treated with DMSO vehicle solvent (Table S1). Caspase activity in response to BG3 exposure has been investigated by staining cells with ApoStat (FITC-conjugated V-D-FMK), which releases green fluorescent rhodamine upon cleavage by caspases. The percentage of *C. albicans* cells stained by V-D-FMK was significantly higher for cells exposed to 1× MIC and 2× MIC of BG3 than that for control cells at 3 h

**Fig. 2** In vitro interaction of bis-guanyldiazones with *C. albicans* chromosomal DNA. (T1–T3 = treatment with decreasing amounts of BG compounds (1000, 400, and 200 μg/mL); C = DMSO treatment; M = molecular marker peqGOLD 1 kb DNA-Ladder Plus)**Fig. 3** In vitro ability of BG3 to interact with double-stranded DNA. **a** CD spectra of DNA treated with BG3. **b** Molecular modeling of BG3 and d(CGCGAATTCGCG)₂

in a dose-dependent manner (Fig. 4c). Levels of metacaspase activity had been comparable in 1× MIC of BG3- and 1× MIC of AmB-treated cells (Fig. 4c).

Effect of BG3 on ROS generation and mitochondrial membrane potential

The analysis of the second marker for apoptosis, ROS generation, and accumulation supported the conclusion that BG3 indeed induced oxidative stress (Fig. 5a). Nevertheless, the ROS generation potential of BG3 was markedly lower in comparison to that of AmB. The amount of ROS generated in 1× MIC of BG3-treated cells was negligible in comparison to control (0.1% DMSO-treated) cells and 28-fold lower in comparison to 1× MIC of AmB treatment. ROS accumulation caused by 2× MIC of BG3 was fourfold lower in comparison

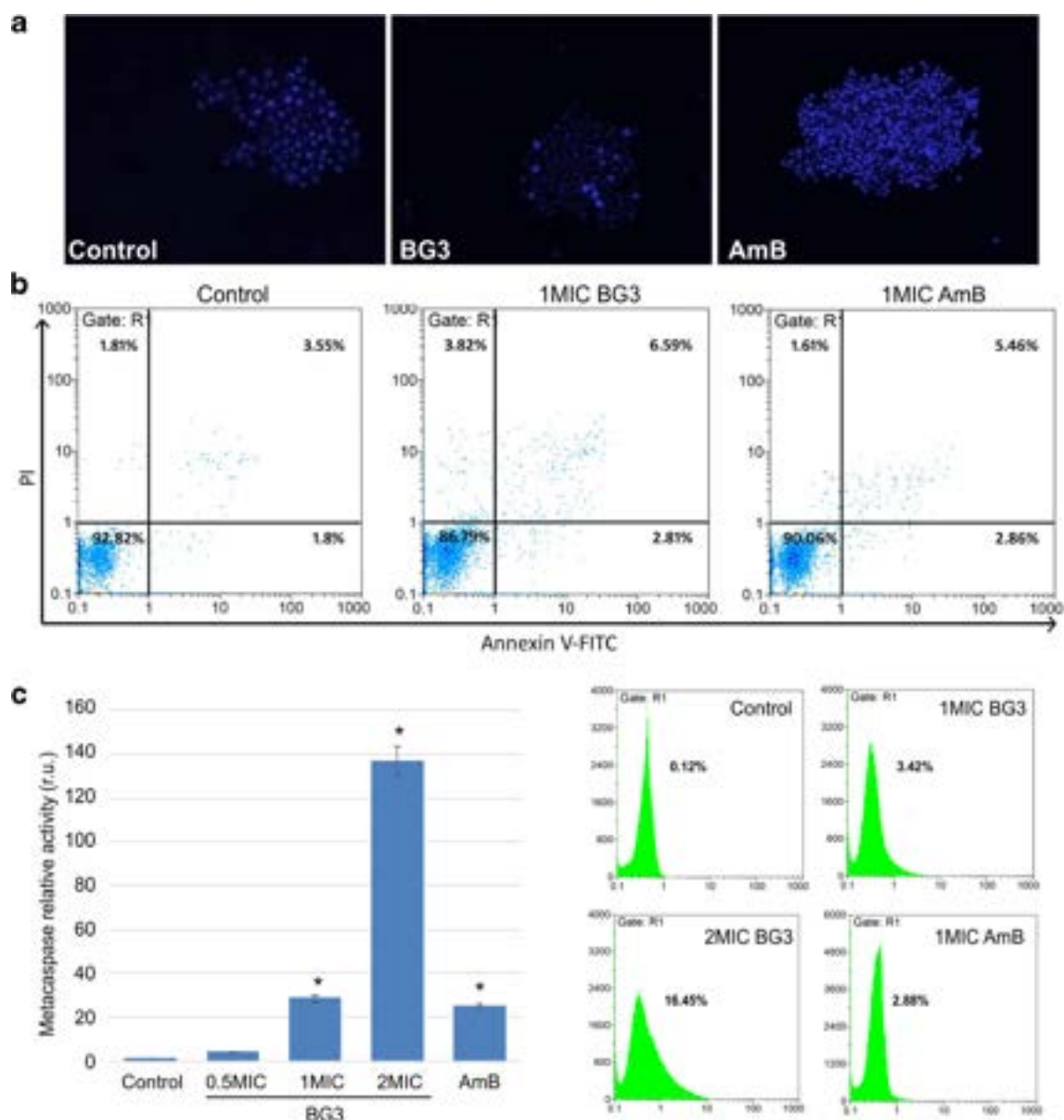


Fig. 4 The pro-apoptotic effect of BG3 on *C. albicans*. **a** DAPI staining was performed after treatment with 1× MIC of each compound for 3 h of incubation (× 60 magnification). **b** Induction of apoptosis in protoplasts by 2× MIC of BG3 and AmB, employing annexin V and propidium

iodide (PI) staining. **c** Metacaspase activity after 0.5× MIC, 1× MIC, and 2× MIC of BG3 and 1× MIC of AmB detected by flow cytometry using FITC-conjugated V-D-FMK for staining. Cells treated with DMSO were used as a control (Control)

to 2× MIC of AmB treatment (Table S2). Indeed, only 2× MIC and higher concentrations of BG3 caused a significant decrease of the ratio of JC-1 aggregate to monomer, interpreted as $\Delta\Psi_m$ depolarization (Fig. 5b), which has crucial impact on the mitochondrial morphology and energy transport. The obvious changes of mitochondrial morphology under a confocal microscope were apparent only at 2× MIC and higher concentration treatment of BG3 (Fig. 5c).

BG3 affected the activities of mitochondrial dehydrogenases assayed by XTT reduction in the dose-dependent manner (Fig. S5a). Relative activity of mitochondrial dehydrogenases treated with 1× MIC and 2× MIC of BG3 were 80 and

55% of the control cells, respectively (Fig. S5a). As mitochondrial dehydrogenases are important in the biosynthesis of ATP, this significant inhibition upon exposure to BG3 may lead to ATP depletion in *C. albicans* mitochondria. On the other side, glutathione reductase and catalase activities under the same treatments were not significantly affected (Fig. S5b).

Effect of BG3 on *C. albicans* SC5314 virulence

In the epithelial infection model, the compound BG3 applied in MIC and sub-MIC successfully reduced hyphal length during the invasion (Fig. 6a, b) and percentage of invading hyphae (18

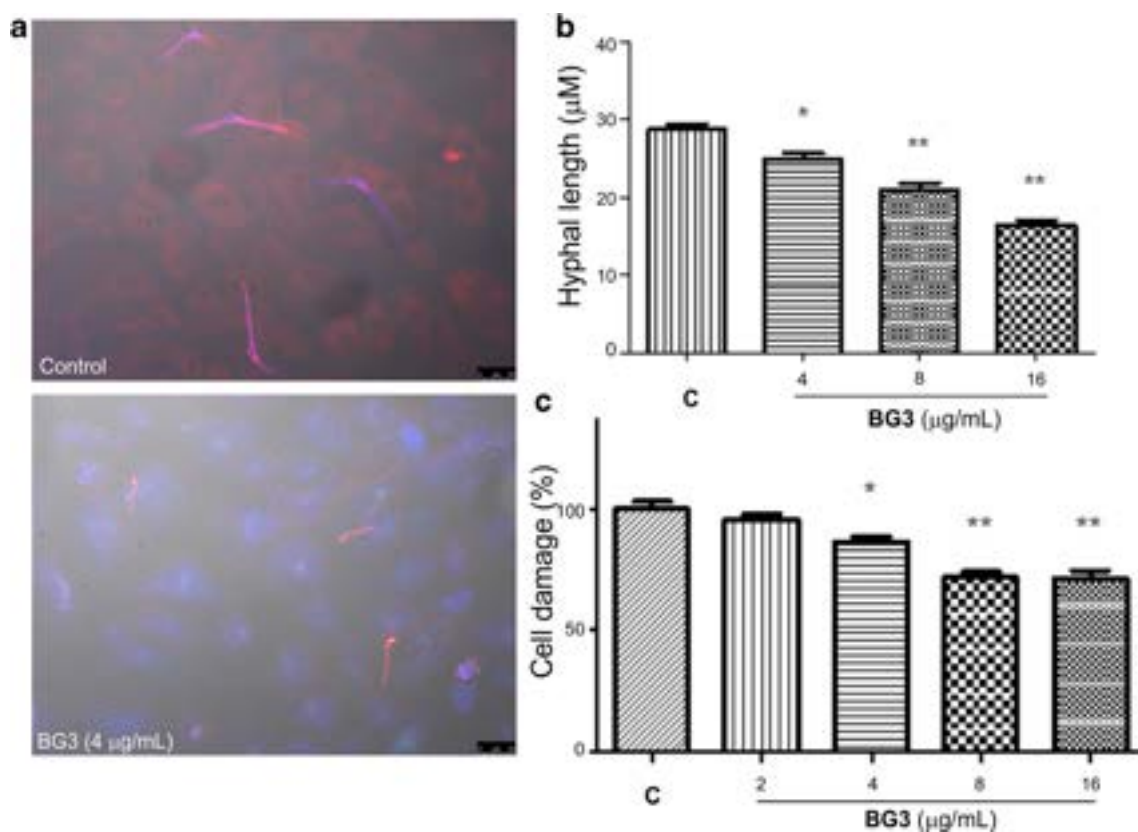


Fig. 6 Effect of BG3 on *C. albicans* SC5314 epithelial infection model. **a** Invasion. **b** Hyphal length. **c** Percent cell damage in comparison to DMSO-treated cells. * $p \leq 0.05$; ** $p \leq 0.01$

thiophene-based guanylhydrazones such as a MIC of 0.25–6.25 µg/mL and favorable toxicity profiles (Ajdačić et al. 2016), especially of the bis-derivative (BG1, Fig. 1), we have generated three novel bis-guanylhydrazones, BG2–BG4 (Fig. 1), to test if the slight modification in the structure could lead to an improvement in antifungal activity and binding affinity to fungal DNA. Indeed, derivatives BG2–BG4 showed improved MIC values in comparison to BG1 against *C. albicans*, with BG3 being the most active against all four species (Table 1). The observed activity was comparable to that of recently reported bis-(*N*-amidinohydrazones) and *N*-(amidino)-*N'*-aryl-bis-hydrazones (Shrestha et al. 2017). Additionally, BG1–4 showed good ability to inhibit the biofilm formation of *C. albicans* (Table 2). Given that the majority of *C. albicans* infections are associated with difficult-to-treat biofilm formation, targeting fungal biofilm formation by small molecules represents a promising new strategy for the development of novel antifungal agents (Tsui et al. 2016; Wu et al. 2017).

It is known that molecules containing cationic amidine and guanidine groups, such as netropsin, distamycin, as well as DAPI, bind to AT-rich sequences in the minor groove of double-stranded DNA and interfere with replication and transcription processes (Bolhuis and Aldrich-Wright 2014; Gowda et al. 2014; Rescifina et al. 2014). Specific interactions

with fungal DNA have not been explored fully as the mode of action of antifungals. Bis-guanylhydrazones from this study showed in vitro DNA binding activity (Figs. 2, 3, and 4 and Fig. S4). Particularly, the oxygen atom of the central cyclic system in BG3 facilitated improved embedding of the molecule to the DNA minor groove, resulting in better DNA interaction of this molecule, while the addition of bulky phenyl group dramatically reduced this interaction in the case of BG4. This specific molecular recognition process has been also shown for antibiotics such as netropsin, and this may be the reason why a certain selectivity has been accomplished with bis-guanylhydrazones towards discrete sequences in fungal DNA that, in turn, influence the transcription of proteins essential for their growth, which was not the case with bacteria (Table 1). Interestingly, BG3 showed the lowest cytotoxicity against human fibroblasts (Table 1).

In fungi, apoptotic-like programmed cell death occurs naturally during aging and can be induced by environmental stresses and exposure to toxic metabolites. It has been demonstrated that *C. albicans* cells undergo apoptosis when exposed to clinically relevant AmB and micafungin (Phillips et al. 2003; Shirazi and Kontoyiannis 2015). Several characteristics of apoptosis, including the exposure of phosphatidylserine at the plasma membrane, DNA degradation, as well as the activation of cysteine-dependent, aspartate-

specific proteases (metacaspases in *Candida* spp.), have been described in fungi (Hao et al. 2013). The appearance of apoptotic markers in *C. albicans* is usually accompanied by the production of ROS, and it was shown that ROS accumulation may be sufficient for inducing apoptosis in *Candida* (Sharon et al. 2009). Mitochondrial aerobic respiratory metabolism plays a major role in *C. albicans* metabolism, and measurement of mitochondrial membrane potential provides information about energy status and cytochrome c release during apoptosis (Gottlieb et al. 2003).

It was previously shown that exposure of *C. albicans* cells to low fungicidal doses of AmB (4–8 µg/mL) produced cellular changes indicative of mammalian apoptosis including ROS accumulation and nuclear fragmentation (Phillips et al. 2003; Tian et al. 2017). We showed that BG3 induced pro-apoptotic effect comparable or higher in comparison to AmB (Fig. 4). Taken together, BG3 interacts with *C. albicans* DNA and provokes killing of *C. albicans* cells by inducing a metacaspase-dependent apoptotic pathway. On the other side, endogenous ROS generation, mitochondrial membrane depolarization, and the levels of activity of oxidative stress-responsive enzymes induced significantly only at 2× MIC and higher concentrations of BG3 indicate that ROS was not the major mediator of BG3-induced apoptosis. Similarly, ROS-independent apoptotic pathway has been described for DNA-interacting gold nanoparticles in *C. albicans* (Seong and Lee 2018).

Invasion of host tissue by *C. albicans* is an important step during the development of candidiasis. However, it has been proposed that the initial epithelial invasion does not elicit host damage, but that *C. albicans* relies on a combination of contact-sensing, directed hyphal extension, active penetration, and the expression of novel pathogenicity factors such as Candidalysin (Moyes et al. 2016) for further inter-epithelial invasion, dissemination, and ultimate damage of host cells (Wachtler et al. 2011, 2012). *C. albicans* strains do not possess the same invasive and virulence properties. SC5314 and ATCC 10231 differ in their ability to invade host tissue and cause experimental infections. Strain SC5314 is invasive whereas strain ATCC 10231 is non-invasive and strongly attenuated in virulence compared to SC5314 (Thewes et al. 2008). It was shown for the first time that BG3 inhibited epithelial cell (TR146) invasion and damage by virulent *C. albicans* SC5314 (Fig. 6).

Antifungal combination therapy has been adopted in the clinic for a long time (Baddley and Pappas 2005). In general, two compounds that interact in a synergistic way most probably exert antimicrobial activity in a different mechanism of action (Agarwal et al. 2012; Musiol et al. 2014). AmB exerts its fungicidal effect by binding to the fungal cell membrane ergosterol moiety and causing porosity on the fungal membrane. Therefore, as BG3 synergistically interacted with AmB, this might indicate that their primary mode of action differs and that the synergistic effects could be attributed to the

combination of two different mechanisms of action, while we have shown that both compounds induce metacaspase-mediated apoptosis. Lowering the dose of clinically relevant AmB has the beneficial effect on both toxicity and the resistance potential.

In this study, four bis-guanylhyazones were generated and characterized in terms of their anti-*Candida* spp. potential. Of these, BG3 stood out for its best in vitro activity, against both growth and biofilm formation, and the lowest toxicity profile. It also showed a synergistic effect with AmB. We propose and show biochemical evidence of selective DNA binding as an initial mode of action of this compound. These findings further illustrate the expanding potential of the guanylhyazone class of compounds, and with further development, BG3 may progress further as a novel mechanism-of-action antifungal agent.

Funding information This work was supported by the Ministry of Education, Science and Technological Development of Serbia (Grant Nos. 172008 and 173048). Research Grant 2015 by the European Society of Clinical Microbiology and Infectious Diseases (ESCMID) to JNR is also acknowledged. Work performed in Jena was funded by the European Union's Horizon 2020 research and innovation program under the Marie Skłodowska-Curie Grant Agreement number 642095 (OPATHY) to MP.

Compliance with ethical standards

Conflict of interest The authors declare that they have no conflict of interest.

Ethical approval This article does not contain any studies with human participants or animals performed by any of the authors.

References

- Agarwal AK, Tripathi SK, Xu T, Jacob MR, Li XC, Clark AM (2012) Exploring the molecular basis of antifungal synergies using genome-wide approaches. *Front Microbiol* 3:115
- Ajdačić V, Senerovic L, Vranić M, Pekmezovic M, Arsic-Arsenijević V, Veselinovic A, Veselinovic J, Šolaja BA, Nikodinovic-Runic J, Opsenica IM (2016) Synthesis and evaluation of thiophene-based guanylhyazones (iminoguanidines) efficient against panel of voriconazole-resistant fungal isolates. *Bioorg Med Chem* 24(6): 1277–1291. <https://doi.org/10.1016/j.bmc.2016.01.058>
- Baddley JW, Pappas PG (2005) Antifungal combination therapy: clinical potential. *Drugs* 65(11):1461–1480. <https://doi.org/10.2165/00003495-200565110-00002>
- Bassetti M, Peghin M, Timsit JF (2016) The current treatment landscape: candidiasis. *J Antimicrob Chemother* 71(suppl 2):ii13–ii22
- Beccia MR, Biver T, Pardini A, Spinelli J, Secco F, Venturini M, Busto Vazquez N, Lopez Comejo MP, Martin Herrera VI, Prado Gotor R (2012) The fluorophore 4',6-diamidino-2-phenylindole (DAPI) induces DNA folding in long double-stranded DNA. *Chem Asian J* 7(8):1803–1810. <https://doi.org/10.1002/asia.201200177>
- Bolhuis A, Aldrich-Wright JR (2014) DNA as a target for antimicrobials. *Bioorg Chem* 55:51–59. <https://doi.org/10.1016/j.bioorg.2014.03.009>

- Brown GD, Denning DW, Gow NA, Levitz SM, Netea MG, White TC (2012a) Hidden killers: human fungal infections. *Sci Transl Med* 4(165):165rv113
- Brown GD, Denning DW, Levitz SM (2012b) Tackling human fungal infections. *Science* 336(6082):647. <https://doi.org/10.1126/science.1222236>
- Calderone R, Sun N, Gay-Andrieu F, Groutas W, Weerawarna P, Prasad S, Alex D, Li D (2014) Antifungal drug discovery: the process and outcomes. *Future Microbiol* 9(6):791–805. <https://doi.org/10.2217/fmb.14.32>
- Clinical and Laboratory Standards Institute (2008) Reference method for broth dilution antifungal susceptibility testing of yeasts—Third Edition: Approved Standard M27-A3. CLSI W, PA, USA
- Clinical and Laboratory Standards Institute (2012) Reference method for broth dilution antifungal susceptibility testing of yeasts: fourth informational supplement M27-S4. CLSI W, PA, USA
- Clinical and Laboratory Standards Institute (2015) Methods for dilution antimicrobial susceptibility tests for bacteria that grow aerobically; Approved Standard—Tenth Edition M07-A10. CLSI W, PA, USA
- Denning DW, Bromley MJ (2015) Infectious disease. How to bolster the antifungal pipeline. *Science* 347(6229):1414–1416. <https://doi.org/10.1126/science.aaa6097>
- Denning DW, Perlin DS, Muldoon EG, Colombo AL, Chakrabarti A, Richardson MD, Sorrell TC (2017) Delivering on antimicrobial resistance agenda not possible without improving fungal diagnostic capabilities. *Emerg Infect Dis* 23(2):177–183. <https://doi.org/10.3201/eid2302.152042>
- Godoy JSR, Kioshima ÉS, Abadio AKR, Felipe MSS, de Freitas SM, Svidzinski TIE (2016) Structural and functional characterization of the recombinant thioredoxin reductase from *Candida albicans* as a potential target for vaccine and drug design. *Appl Microbiol Biotechnol* 100(9):4015–4025. <https://doi.org/10.1007/s00253-015-7223-8>
- Gottlieb E, Armour SM, Harris MH, Thompson CB (2003) Mitochondrial membrane potential regulates matrix configuration and cytochrome c release during apoptosis. *Cell Death Differ* 10(6):709–717. <https://doi.org/10.1038/sj.cdd.4401231>
- Gowda KRS, Mathew BB, Sudhamani CN, Naik HSB (2014) Mechanism of DNA binding and cleavage. *Biomed Biotechnol* 2:1–9
- Guinea J (2014) Global trends in the distribution of *Candida* species causing candidemia. *Clin Microbiol Infect* 20:5–10. <https://doi.org/10.1111/1469-0691.12539>
- Guo H, Xie SM, Li SX, Song YJ, Lv XL, Zhang H (2014) Synergistic mechanism for tetrandrine on fluconazole against *Candida albicans* through the mitochondrial aerobic respiratory metabolism pathway. *J Med Microbiol* 63(Pt 7):988–996. <https://doi.org/10.1099/jmm.0.073890-0>
- Hansen MB, Nielsen SE, Berg K (1989) Re-examination and further development of a precise and rapid dye method for measuring cell growth/cell kill. *J Immunol Methods* 119(2):203–210. [https://doi.org/10.1016/0022-1759\(89\)90397-9](https://doi.org/10.1016/0022-1759(89)90397-9)
- Hao B, Cheng S, Clancy CJ, Nguyen MH (2013) Caspofungin kills *Candida albicans* by causing both cellular apoptosis and necrosis. *Antimicrob Agents Chemother* 57(1):326–332. <https://doi.org/10.1128/AAC.01366-12>
- Hazen KC, Lay JG, Hazen BW, RC F, Murthy S (1990) Partial biochemical characterization of cell surface hydrophobicity and hydrophilicity of *Candida albicans*. *Infect Immun* 58(11):3469–3476
- Jakab A, Mogavero S, Forster TM, Pekmezovic M, Jablonowski N, Dombradi V, Pocsí I, Hube B (2016) Effects of the glucocorticoid betamethasone on the interaction of *Candida albicans* with human epithelial cells. *Microbiology* 162(12):2116–2125
- Kathiravan MK, Salake AB, Chothe AS, Dudhe PB, Watode RP, Mukta MS, Gadhwane S (2012) The biology and chemistry of antifungal agents: a review. *Bioorg Med Chem* 20(19):5678–5698. <https://doi.org/10.1016/j.bmc.2012.04.045>
- Maiolo EM, Furustrand Tafin U, Borens O, Trampuz A (2014) Activities of fluconazole, caspofungin, anidulafungin, and amphotericin B on planktonic and biofilm *Candida* species determined by microcalorimetry. *Antimicrob Agents Chemother* 58(5):2709–2717. <https://doi.org/10.1128/AAC.00057-14>
- Morris GM, Huey R, Lindstrom W, Sanner MF, Belew RK, Goodsell DS, Olson AJ (2009) AutoDock4 and AutoDockTools4: automated docking with selective receptor flexibility. *J Comput Chem* 30(16):2785–2791. <https://doi.org/10.1002/jcc.21256>
- Moyes DL, Wilson D, Richardson JP, Mogavero S, Tang SX, Wemecke J, Höfs S, Gratacap RL, Robbins J, Runglall M, Murciano C, Blagojevic M, Thavaraj S, Förster TM, Hebecker B, Kasper L, Vizcay G, Iancu SI, Kichik N, Häder A, Kurzai O, Luo T, Krüger T, Kniemeyer O, Cota E, Bader O, Wheeler RT, Gutsmann T, Hube B, Naglik JR (2016) Candidalysin is a fungal peptide toxin critical for mucosal infection. *Candidalysin is a fungal peptide toxin critical for mucosal infection. Nature* 532(7597):64–68. <https://doi.org/10.1038/nature17625>
- Musiol R, Mrozek-Wilczkiewicz A, Polanski J (2014) Synergy against fungal pathogens: working together is better than working alone. *Curr Med Chem* 21(7):870–893. <https://doi.org/10.2174/0929867321666131218094848>
- Ngo HX, Gameau-Tsodikova S, Green KD (2016) A complex game of hide and seek: the search for new antifungals. *Med Chem Commun* 7(7):1285–1306. <https://doi.org/10.1039/C6MD00222F>
- Odds FC (2003) Synergy, antagonism, and what the checkerboard puts between them. *J Antimicrob Chemother* 52(1):1. <https://doi.org/10.1093/jac/dkg301>
- Ostrosky-Zeichner L, Casadevall A, Galgiani JN, Odds FC, Rex JH (2010) An insight into the antifungal pipeline: selected new molecules and beyond. *Nat Rev Drug Discov* 9(9):719–727. <https://doi.org/10.1038/nrd3074>
- Perfect JR (2017) The antifungal pipeline: a reality check. *Nat Rev Drug Discov* 16(9):603–616. <https://doi.org/10.1038/nrd.2017.46>
- Phillips AJ, Sudbery I, Ramsdale M (2003) Apoptosis induced by environmental stresses and amphotericin B in *Candida albicans*. *PNAS* 100(24):14327–14332. <https://doi.org/10.1073/pnas.2332326100>
- Pierce CG, Uppuluri P, Tristan AR, Wornley FL Jr, Mowat E, Ramage G, Lopez-Ribot JL (2008) A simple and reproducible 96-well plate-based method for the formation of fungal biofilms and its application to antifungal susceptibility testing. *Nat Protoc* 3(9):1494–1500. <https://doi.org/10.1038/nprot.2008.141>
- Rescificina A, Zagni C, Varrica MG, Pistrà V, Corsaro A (2014) Recent advances in small organic molecules as DNA intercalating agents: synthesis, activity, and modeling. *Eur J Med Chem* 74:95–115. <https://doi.org/10.1016/j.ejmech.2013.11.029>
- Rowan R, McCann M, Kavanagh K (2010) Analysis of the response of *Candida albicans* cells to silver(I). *Med Mycol* 48(3):498–505. <https://doi.org/10.3109/13693780903222513>
- Sanner MF (1999) Python: a programming language for software integration and development. *J Mol Graph Model* 17(1):57–61
- Scorzoni L, de Paula ESAC, Marcos CM, Assato PA, de Melo WC, de Oliveira HC, Costa-Orlandi CB, Mendes-Giannini MJ, Fusco-Almeida AM (2017) Antifungal therapy: new advances in the understanding and treatment of mycosis. *Front Microbiol* 8:36
- Seong M, Lee DG (2018) Reactive oxygen species-independent apoptotic pathway by gold nanoparticles in *Candida albicans*. *Microbiol Res* 207(supplement C):33–40
- Sharon A, Finkelstein A, Shlezinger N, Hatam I (2009) Fungal apoptosis: function, genes and gene function. *FEMS Microbiol Rev* 33(5):833–854. <https://doi.org/10.1111/j.1574-6976.2009.00180.x>
- Shirazi F, Kontoyiannis DP (2015) Micafungin triggers caspase-dependent apoptosis in *Candida albicans* and *Candida parapsilosis* biofilms, including caspofungin non-susceptible isolates. *Virulence* 6(4):385–394. <https://doi.org/10.1080/21505594.2015.1027479>

- Shrestha SK, Kril LM, Green KD, Kwiatkowski S, Sviripa VM, Nickell JR, Dwoskin LP, Watt DS, Garneau-Tsodikova S (2017) Bis(N-amidinohydrazones) and N-(amidino)-N'-aryl-bishydrazones: new classes of antibacterial/antifungal agents. *Bioorg Med Chem* 25(1): 58–66. <https://doi.org/10.1016/j.bmc.2016.10.009>
- Silva S, Negri M, Henriques M, Oliveira R, Williams DW, Azeredo J (2012) *Candida glabrata*, *Candida parapsilosis* and *Candida tropicalis*: biology, epidemiology, pathogenicity and antifungal resistance. *FEMS Microbiol Rev* 36(2):288–305. <https://doi.org/10.1111/j.1574-6976.2011.00278.x>
- Thewes S, Moran GP, Magee BB, Schaller M, Sullivan DJ, Hube B (2008) Phenotypic screening, transcriptional profiling, and comparative genomic analysis of an invasive and non-invasive strain of *Candida albicans*. *BMC Microbiol* 8(1):187. <https://doi.org/10.1186/1471-2180-8-187>
- Tian H, Qu S, Wang Y, Lu Z, Zhang M, Gan Y, Zhang P, Tian J (2017) Calcium and oxidative stress mediate perillaldehyde-induced apoptosis in *Candida albicans*. *Appl Microbiol Biotechnol* 101(8): 3335–3345. <https://doi.org/10.1007/s00253-017-8146-3>
- Trott O, Olson AJ (2010) AutoDock Vina: improving the speed and accuracy of docking with a new scoring function, efficient optimization, and multithreading. *J Comput Chem* 31(2):455–461
- Tsui C, Kong EF, Jabra-Rizk MA (2016) Pathogenesis of *Candida albicans* biofilm. *Pathog Dis* 74(4):ftw018
- Uppuluri P, Srinivasan A, Ramasubramanian A, Lopez-Ribot J (2011) Effects of fluconazole, amphotericin B, and Caspofungin on *Candida albicans* biofilms under conditions of flow and on biofilm dispersion. *Antimicrob Agents Chemother* 55(7):3591–3593. <https://doi.org/10.1128/AAC.01701-10>
- van der Meer JWM, van de Veerdonk FL, Joosten LAB, Kullberg B-J, Netea MG (2010) Severe *Candida* spp. infections: new insights into natural immunity. *Int J Antimicrob Agents* 36:S58–S62. <https://doi.org/10.1016/j.ijantimicag.2010.11.013>
- Wachtler B, Wilson D, Haedicke K, Dalle F, Hube B (2011) From attachment to damage: defined genes of *Candida albicans* mediate adhesion, invasion and damage during interaction with oral epithelial cells. *PLoS One* 6(2):e17046. <https://doi.org/10.1371/journal.pone.0017046>
- Wachtler B, Citiulo F, Jablonowski N, Forster S, Dalle F, Schaller M, Wilson D, Hube B (2012) *Candida albicans*-epithelial interactions: dissecting the roles of active penetration, induced endocytosis and host factors on the infection process. *PLoS One* 7(5):e36952. <https://doi.org/10.1371/journal.pone.0036952>
- Wei D, Wilson WD, Neidle S (2013) Small-molecule binding to the DNA minor groove is mediated by a conserved water cluster. *J Am Chem Soc* 135(4):1369–1377. <https://doi.org/10.1021/ja308952y>
- Wu XZ, Cheng AX, Sun LM, Sun SJ, Lou HX (2009) Plagiochin E, an antifungal bis(bibenzyl), exerts its antifungal activity through mitochondrial dysfunction-induced reactive oxygen species accumulation in *Candida albicans*. *Biochim Biophys Acta* 1790:770–777
- Wu XZ, Chang WQ, Cheng AX, Sun LM, Lou HX (2010) Plagiochin E, an antifungal active macrocyclic bis(bibenzyl), induced apoptosis in *Candida albicans* through a metacaspase-dependent apoptotic pathway. *Biochim Biophys Acta* 1800(4):439–347. <https://doi.org/10.1016/j.bbagen.2010.01.001>
- Wu S, Wang Y, Liu N, Dong G, Sheng C (2017) Tackling fungal resistance by biofilm inhibitors. *J Med Chem* 60(6):2193–2211. <https://doi.org/10.1021/acs.jmedchem.6b01203>